https://doi.org/10.5194/egusphere-2026-841
Preprint. Discussion started: 17 June 2026

Regional Variations in Drivers of Active Layer Thickness: A Site-Scale Analysis Across Northern Hemisphere Permafrost

Yutong Lin, Bo Zhang and Haoqi Suo, Meng Guo *

Key Laboratory of Geographical Processes and Ecological Security in Changbai Mountains, Ministry of Education, School of Geographical Sciences, Northeast Normal University, Changchun 130024, China

**Corresponding author*

Email: guom521@nenu.edu.cn

Abstract: In recent decades, permafrost degradation across the Northern Hemisphere has accelerated markedly under climate warming. However, the characteristics and driving mechanisms of this degradation at the sample-plot scale remain poorly understood. This study classifies Northern Hemisphere permafrost into three types: the Circum-Arctic permafrost region (CAP), the Sub-Circum-Arctic permafrost region (SCAP), and the Qinghai–Tibet Plateau (QTP) permafrost region. Based on data from 785 active layer thickness (ALT) monitoring sites we found that the mean value of ALT in CAP, SCAP and QTP region was 84.9 ± 1.56 cm, 200 ± 8.99 cm and 224 ± 7.26 cm, respectively. Based on 291 sites with more than five years of ALT records, we found that 60% of the sites exhibit an increasing trend in ALT (35% with statistically significant increases), while 40% show a decreasing trend (11% with statistically significant decreases). The rates of ALT changing vary considerably among different permafrost regions and with higher increasing rate in QTP (3.23 cm yr^{-1}, n=36) and followed by CAP (1.48 cm yr^{-1}, n=58) and SCAP (1.19 cm yr^{-1}, n=38). Results from the Partial least squares path modelling (PLS-PM) indicate that, at the site scale, soil characteristics exert a stronger influence on ALT than air temperature, particularly in the CAP and QTP regions. In SCAP, precipitation is the most important factor driving ALT changes, as higher precipitation can transfer heat into the soil and affect soil temperature. Vegetation also plays a significant role in SCAP, where denser vegetation can generate a warming effect. Snow cover shows limited influence on ALT across all monitoring sites. This study offers a systematic review of permafrost degradation and its driving mechanisms at the monitoring-site scale.

Keywords: Active layer thickness; ALT monitoring site; Soil properties; Site scale; PLS-PM

https://doi.org/10.5194/egusphere-2026-841
Preprint. Discussion started: 17 June 2026

1 Introduction

Permafrost, a vital component of the Earth's cryosphere, refers to soil or rock that remains frozen for at least two consecutive years (Heginbottom, 2002; Jin et al., 2021). It covers approximately 15-17% of the Northern Hemisphere's land surface, spanning high-latitude and high-altitude regions, and plays a critical role in regulating ecosystem functions and climate dynamics (Obu, 2021). However, in recent decades, widespread permafrost degradation has been observed, with profound implications for both local ecosystems and global processes, particularly through its impact on carbon storage and release (Smith et al., 2022). The Arctic permafrost is especially vulnerable, as warming in this region occurs at a rate faster than the global average (Rantanen et al., 2024). While understanding the characteristics of regional permafrost degradation is critical for reducing uncertainties in future projections and designing effective climate strategies, but the specific features of these degradation processes and their regional variations remain poorly understood.

The active layer, located above the permafrost, thaws during warmer months and refreezes in winter (Dobinski, 2011), serving as a critical interface for energy and mass exchange between the permafrost, pedosphere, and atmosphere (Luo et al., 2023). Influenced by multiple factors, active layer thickness (ALT) — the most common and objectively quantifiable indicator of permafrost degradation — has exhibited a pronounced increasing trend over the past several decades, though the magnitude of this increase varies across regions (Peng et al., 2023; Shen et al., 2023). As the active layer provides essential water and nutrients to sustain biological activity and vegetation growth in permafrost regions (Berner et al., 2020; Luo et al., 2023), changes in ALT can profoundly impact ecological processes in cold-region

https://doi.org/10.5194/egusphere-2026-841
Preprint. Discussion started: 17 June 2026

ecosystems (Reyes and Lougheed, 2015). Permafrost regions can be categorized into high-latitude, mid-to-high latitude, high-altitude, and mid-to-low altitude zones, with ALT characteristics and driver mechanisms differing across these types (Yang et al., 2024). Despite being the most common and objectively quantifiable indicator of permafrost degradation, the spatial patterns and regional characteristics of ALT variation remain poorly understood, hindering a deeper elucidation of its impact mechanisms across different regions.

The response of ALT to climate warming varies significantly among regions due to complex interactions between soil, vegetation, snowpack, and topography (Jorgenson et al., 2010). Extensive research on the driving factors of ALT has been conducted over the past several decades, spanning plot, regional, and global scales. However, results and conclusions have not always been consistent across different spatial scales and regions (Peng et al., 2023). At the regional or global scale, air temperature and solar radiation are the dominant factors influencing ALT while at the local scale, topography, vegetation cover, soil properties, and disturbances play crucial roles by modulating soil thermal properties and the surface energy balance in various ways (Guglielmin et al., 2014; Luo et al., 2023). Current understanding of the driving mechanisms behind ALT variations remains inadequate, and it remains unclear whether these mechanisms differ across diverse permafrost types.

The limited availability of field surveys and long-term monitoring data poses significant challenges to understanding ALT dynamics at site scale. Much existing research relies on remote sensing and predictive models (Anthony et al., 2018; Berner et al., 2020), which often produce coarse spatial resolution maps. Field-based studies are generally restricted to fine scales and short timeframes (Du et al., 2022). To address these limitations, the Circumpolar Active Layer Monitoring (CALM) network and the Global Terrestrial Network for Permafrost (GTN-P) have provided

https://doi.org/10.5194/egusphere-2026-841
Preprint. Discussion started: 17 June 2026

point-measured ALT data from 305 sites since the 1990s. These datasets serve as valuable tools for validating large-scale ALT estimates derived from remote sensing and climate models (Yang et al., 2024) and hold potential for understanding the driving factors of permafrost degradation at the site scale. However, current summary and deeply analysis of these data products remain insufficient, and no consistent conclusions of ALT variety and driving mechanisms have been reached.

Building on these research gaps, this study aims to advance understanding of ALT variability trends and driving mechanisms across diverse permafrost regions, using extensive ALT site monitoring data and additional sites from relevant literature. To achieve this, we divided the Northern Hemisphere's permafrost regions into the Circum-Arctic permafrost region (CAP), the Sub-Circum-Arctic permafrost region (SCAP) based on permafrost continuity and location. Considering the distinct altitude-driven characteristics of permafrost on the Qinghai–Tibet Plateau (QTP), this region was analyzed separately. The specific objectives of this study are to (1) clarify the general characteristics of ALT in different permafrost zones; (2) elucidate the multi-year variation trends of ALT at each monitoring site; and (3) identify the relative importance of environmental factors and the driving mechanisms of ALT changes in diverse permafrost regions. These insights will contribute to refining predictive models of permafrost degradation and guiding effective adaptation and mitigation strategies under global climate change.

2 Materials and methods

2.1 Study regions

In the Northern Hemisphere, permafrost is primarily distributed in the Arctic, subarctic, plateaus, and mountainous areas. Based on continuity, permafrost is

https://doi.org/10.5194/egusphere-2026-841
Preprint. Discussion started: 17 June 2026

classified into four types: continuous permafrost (>90%), discontinuous permafrost (50%-90%), sporadic permafrost (10%-50%), and isolated patches (0%-10%) (Brown et al., 1997). As a distinct mid-latitude geographical entity, the permafrost on the Qinghai-Tibet Plateau (QTP) is predominantly elevation-dependent. Additionally, unlike other permafrost regions, the QTP is dominated by bare land (46.56%) and grassland (43.26%) (Wu and Zhang, 2010). Therefore, the QTP permafrost region was treated as an independent research area in this study. Overall, the Northern Hemisphere permafrost was categorized into three groups: Based on the spatial distribution characteristics and degree of continuity across different permafrost-zone types, as well as the distribution of ALT sites within these zones, we merged the generic permafrost categories into three regions: the Circum-Arctic permafrost region (CAP, the same as continuous permafrost in Brown et al. (1997)), the sub–Circum-Arctic permafrost region (SCAP, including discontinuous, sporadic, and isolated patches), and the Qinghai–Tibet Plateau (QTP) permafrost region (Fig. 1).

https://doi.org/10.5194/egusphere-2026-841
Preprint. Discussion started: 17 June 2026

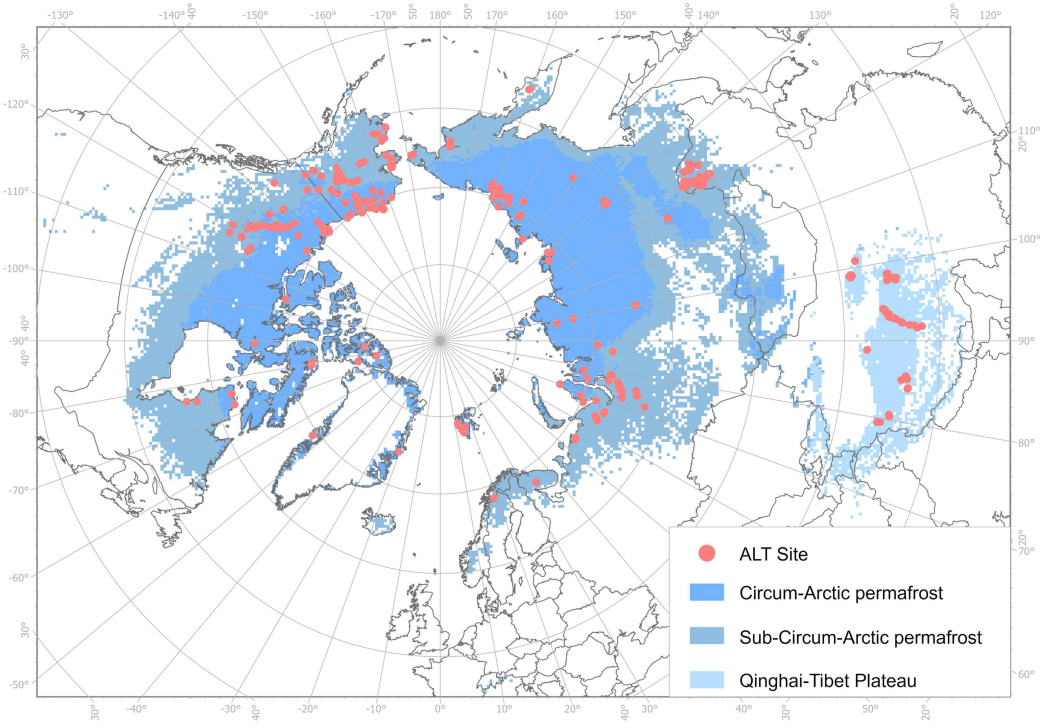

Fig. 1 Location of ALT sites and the permafrost types used in this study. Permafrost regions classification are based on *Brown et al. (1997) and Obu et al. (2021).*

2.2 ALT data collection

The ALT data utilized in this study were obtained from the Circumpolar Active Layer Monitoring (CALM) ,comprising 243 sites (Shiklomanov et al., 2008); the Global Terrestrial Network for Permafrost (GTN-P) database from which 406 borehole sites with ALT records were extracted (Biskaborn et al., 2015), and published literature,yielding an additional 136 sites (Supplementary Information). Literature-derived data included field measurements collected using steel rods, pitting, drilling, ground-penetrating radar, and thaw tubes. In some cases, ALT was estimated from the depth of the 0 °C isotherm. To ensure data reliability, local vegetation

https://doi.org/10.5194/egusphere-2026-841
Preprint. Discussion started: 17 June 2026

characteristics and historical disturbance conditions were examined, and sites affected by fire were excluded. All ALT records represent the annual maximum thaw depth, typically observed in September or October.

To improve the accuracy of ALT trend analysis, all selected data underwent rigorous screening and quality control following the methodology of Liu et al. (2024). Ultimately, 250 ALT sites in the CAP region, 228 in the SCAP region, and 307 on the QTP were retained for further analysis. Among the 785 sites, 219 (104 in the CAP, 79 in the SCAP, and 36 on the QTP) with more than five consecutive years of observations were used for the site-level trend analysis.

2.3 Environmental data

The environmental datasets used in this study were categorized into four groups: meteorological, vegetation, topographic, and soil data (Table 1). Growing Degree Days (GDD) were calculated as the cumulative sum of daily mean temperatures above 0 ℃ (℃ · day). Growing Season Temperature (GST) was defined as the mean temperature during the growing season (April – October). Net solar radiation (RNS) was derived from monthly data and averaged to annual values. For snow cover, three variables were derived for the period from the previous November to April: snow cover days (SCD), average snow depth (SD), and total annual snowfall (SNF).

The Topographic Wetness Index (TWI), calculated from a Digital Elevation Model (DEM), is a terrain-based metric that quantifies the spatial distribution of surface soil moisture by integrating the contributing catchment area and local drainage conditions.

All climate data processing was performed using the Google Earth Engine (GEE) platform. Meteorological, vegetation, topographic, and soil variables were extracted at each ALT site and used for subsequent analyses.

https://doi.org/10.5194/egusphere-2026-841
Preprint. Discussion started: 17 June 2026

Table 1 The data used in this study

Data category	Data name	Data meaning	Data information
Climate	MAT	Mean Annual air Temperature	ERA5-Land monthly averaged data with a spatial resolution of 0.1 degrees (Muñoz-Sabater, 2019)
	LST	Mean Annual Land Surface Temperature	
	GDD	Annual Growing Degree Days	ECMWF/ERA5-Land Daily Aggregated data with a spatial resolution of 0.1 degrees (Muñoz Sabater et al., 2024)
	GST	Mean Growing Season Temperature	
	RNS	Net solar radiation	
	SD	Mean Annual Snow Depth of the former winter	
	SNF	Total annual snowfall of the former winter	
	SCD	Total annual snow cover days of the former winter	
	TP	Total annual precipitation	ERA5-Land monthly averaged data with a spatial resolution of 0.1 degrees (Muñoz-Sabater, 2019)
Vegetation	NDVI	Mean annual Normalized Difference Vegetation Index	GIMMS NDVI3g dataset featuring a temporal resolution of 15 days and a spatial resolution of 8 km (Pinzon and Tucker, 2014)
Topography	Elev	Elevation	ASTER GDEM V3 with a spatial resolution of 30 meters (NASA et al., 2018)
	Asp	Aspect	
	Slope	Slope	
	TWI	Topographic Wetness Index	Calculated based on the DEM; derived by extracting flow accumulation and slope
Soil	Dsoil	Soil Depth	Derived from the Soil Grids 250m 2017 - 03 dataset of ISRIC - World Soil Information (Hengl et al., 2017)
	SSC	Soil Sand Content	Harmonized World Soil Database v2.0 (FAO and IIASA, 2023)
	SWC	Soil Water Content (0-7cm)	ERA5-Land monthly averaged data (Muñoz-Sabater, 2019)
	SWC2	Soil Water Content (7-28cm)	
	SWC3	Soil Water Content (28-100cm)	

2.4 Statistical analysis

2.4.1 Linear trend analysis of ALT

Least squares linear regression analysis was applied to calculate the linear trends of ALT at sites with more than 5 years of continuous monitoring data. The significance of linear trends was assessed using two-tailed t-tests, with a *p-value* < 0.05 considered statistically significant.

https://doi.org/10.5194/egusphere-2026-841
Preprint. Discussion started: 17 June 2026

2.4.2 Correlation analysis

Spearman's correlation analyses were performed to explore the relationships between ALT and potential influencing factors for each individual site-year. Two-tailed significance tests were used to evaluate correlation significance, with *p-value* < 0.05 indicating a statistically significant correlation.

2.4.3 Multicollinearity diagnostic

To assess potential multicollinearity among the predictor variables, we conducted diagnostics using the Variance Inflation Factor (VIF). The VIF measures how much the variance of an estimated regression coefficient is inflated because a predictor is correlated with other predictors in the model. Larger VIF values therefore indicate stronger multicollinearity, which can reduce the stability of coefficient estimates and hinder clear interpretation of individual predictor effects. Consistent with commonly used guidelines in statistical modelling, VIF values greater than 10 were taken to reflect severe multicollinearity in this study (Marquardt, 1970).

2.4.4 Extreme Gradient Boosting (XGBoost) model

Extreme Gradient Boosting (XGBoost) is an optimized implementation of the gradient boosting framework (Chen and Guestrin, 2016). widely recognized for its high speed and superior accuracy in supervised learning tasks (e.g., classification, regression, ranking). XGBoost pushes boosted trees to their computational potential, delivering both high-speed performance and superior accuracy. Compared with traditional gradient boosting methods, XGBoost incorporates key enhancements, including a second-order Taylor expansion of the loss function that utilizes second-order derivatives to accelerate convergence during training. In this study, the XGBoost model was employed to rank the relative importance of environmental

https://doi.org/10.5194/egusphere-2026-841
Preprint. Discussion started: 17 June 2026

factors influencing ALT.The XGBoost model was trained using a 70%/30% random split for training and validation (random_state = 42). Key hyperparameters were set as follows: learning rate = 0.1, maximum tree depth = 3, subsample ratio = 0.8, column subsample ratio = 0.8, and number of boosting rounds = 100. Model performance was evaluated using R^2 and RMSE on the validation set.

2.4.5 Partial least squares path modelling (PLS-PM)

Partial least squares path modelling (PLS-PM) is a flexible multivariate analytical framework widely recognized for its strong predictive capability and its relatively relaxed assumptions regarding data distribution and model complexity. In PLS-PM, variable relationships are represented through a causal network consisting of a structural model (specifying directional links among latent variables) and a measurement model (defining how latent variables are operationalized via observed indicators). The core objective of PLS-PM is to maximize the explained variance (R^2) of endogenous latent variables, making it particularly suitable for prediction-oriented research and identifying key mechanisms underlying system behaviour. Notably, PLS-PM does not require strict multivariate normality, enabling effective application to heterogeneous or non-normally distributed dat (Hair et al., 2019). In this study, PLS-PM was used to investigate the driving factors of ALT variations across different research regions (Tenenhaus et al., 2005).

3 Results

3.1 ALT in different permafrost regions

From 1990 to 2021, the mean ALT on the QTP was 224 ± 7.26 cm, which was higher than that in the SCAP (200 ± 8.99 cm). The CAP showed the smallest average

https://doi.org/10.5194/egusphere-2026-841
Preprint. Discussion started: 17 June 2026

ALT (84.9 ± 1.56 cm). (Fig. 2). In terms of distribution patterns, ALT in the CAP generally exhibited a normal distribution, with most values concentrated between 50 and 100 cm. ALT in the SCAP was primarily distributed between 50 and 130 cm. It should be noted that the SCAP in this study also includes scattered and isolated permafrost patches located at the southern margin of the Northern Hemisphere permafrost zone Brown et al. (1997), which explains why ALT occasionally exceeds 500 cm. On the QTP, ALT displayed three distinct peaks (approximately 160 cm, 230 cm, and 310 cm), and maximum values also exceeded 500 cm. This multimodal pattern reflects the coexistence of diverse permafrost types across the region (Brown et al. 1997).

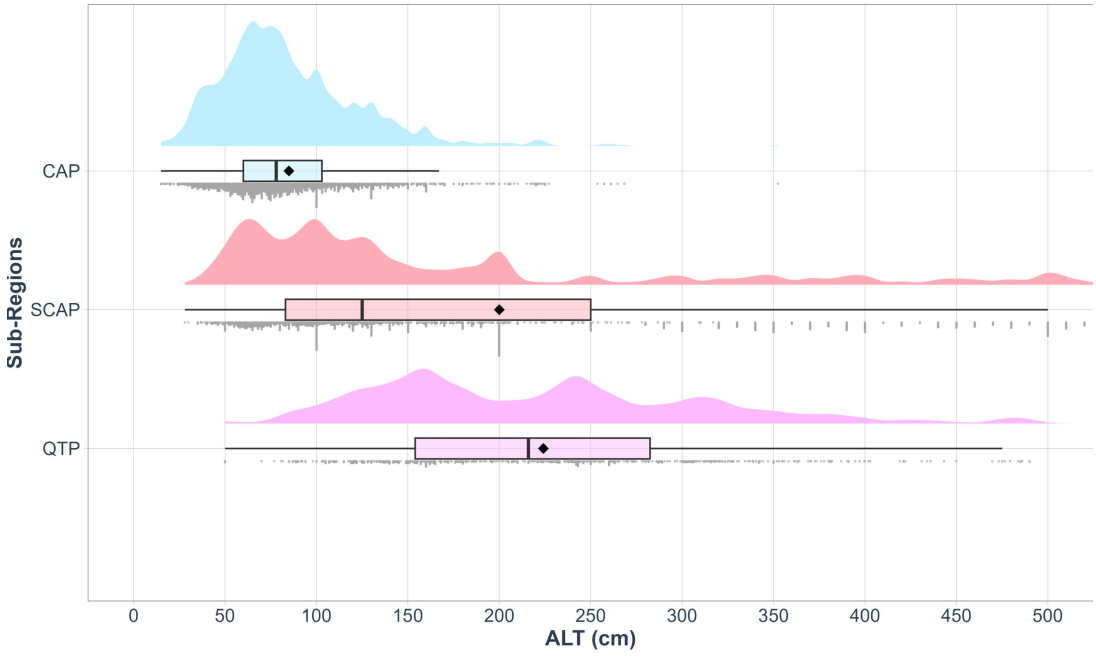

Fig. 2 The histograms of active layer thickness (ALT) in the Circum-Arctic permafrost region (CAP), the Sub-Circum-Arctic permafrost region (SCAP), and the Qinghai–Tibet Plateau (QTP) permafrost region

https://doi.org/10.5194/egusphere-2026-841
Preprint. Discussion started: 17 June 2026

3.2 The ALT trend at site level within different permafrost regions

Among the 219 sites with more than 5 years of continuous ALT observations, 132 sites (60%) exhibited an increasing trend in ALT while 87 sites (40%) showed a decreasing trend. Specifically, 76 sites (35%) showed a significantly increasing trend ($p < 0.05$), whereas 25 sites (11%) showed a significantly decreasing trend, indicating overall permafrost degradation (ALT thickening) across much of the Northern Hemisphere, although the rate and direction of change varied by permafrost type.

In the CAP, 63% of the sites (66 sites) showed a decreasing ALT trend and 37% (38 sites) showed an increasing trend. However, the number of sites with significantly increasing ALT (17 sites) slightly exceeded those with significantly decreasing ALT (14 sites). In contrast, increasing ALT dominated both the SCAP and QTP, and all monitored sites on the QTP exhibited ALT thickening.

Regarding the rate of increase, the QTP experienced the fastest ALT thickening, with a mean rate of (3.23 $cm \cdot yr^{-1}$, $n = 36$), followed by the CAP (1.48 $cm \cdot yr^{-1}$, $n = 38$) and the SCAP (1.19 $cm \cdot yr^{-1}$, $n = 58$). Among sites with significantly increasing ALT, the QTP again showed the highest rate (4.13 $cm \cdot yr^{-1}$, $n = 20$), whereas the CAP and SCAP exhibited substantially lower but comparable rates (1.50 $cm \cdot yr^{-1}$, $n = 17$; and 1.49 $cm \cdot yr^{-1}$, $n = 39$, respectively). These results demonstrate that ALT increases are more common in the SCAP and QTP, indicating more widespread and pronounced permafrost degradation in these regions.

https://doi.org/10.5194/egusphere-2026-841
Preprint. Discussion started: 17 June 2026

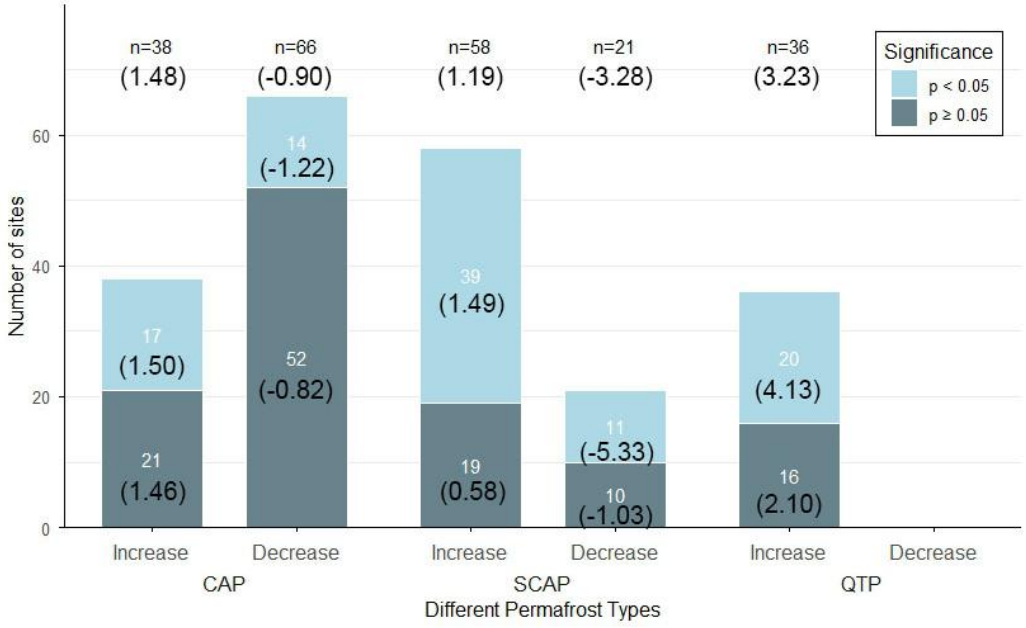

Fig. 3 The active layer thickness (ALT) site number of increasing and decreasing trend in the Circum-Arctic permafrost region (CAP), the Sub-Circum-Arctic permafrost region (SCAP), and the Qinghai–Tibet Plateau (QTP) permafrost region. The numbers in parentheses denote the mean annual rate of change for ALT, with units expressed as cm yr^{-1}; the number above the parentheses is the site number.

3.3 Relationships between ALT and environmental factors

The VIF diagnostics confirmed that RNS was highly collinear with these core thermal variables. Its VIF value exceeded the threshold of 10 in the discontinuous permafrost zone (reaching 11.15). Similarly, deeper soil moisture variables (SWC2 and SWC3) were excluded from the models due to severe multicollinearity, as evidenced by extremely high VIF values across all study regions. Specifically, VIFs reached 181.16 for SWC2 and 133.24 for SWC3 in the CAP; 415.75 and 259.16 in the SCAP; and 374.88 and 214.84 in the QTP. Given their physical redundancy and the availability of a more direct surface-layer indicator, only SWC was retained in the

https://doi.org/10.5194/egusphere-2026-841
Preprint. Discussion started: 17 June 2026

final models, as it sufficiently captures the soil hydrological conditions relevant to active layer dynamics.

The relationships between ALT and the environmental factors (Fig. 4) indicate that, in the CAP, the ALT shows the closed correlation with SWC ($r = 0.40^{***}$), followed by GST ($r = 0.36^{***}$), MAT ($r = 0.35^{***}$), and LST (r = 0.33***), while no significant correlations are observed with NDVI, TWI, and SCD. In the SCAP, ALT exhibits the highest correlation with Dsoil ($r = 0.47^{***}$), followed by the topographic factors of Elev ($r = -0.33^{***}$), Asp ($r = -0.31^{***}$), and Slope ($r = -0.28^{***}$). Across the QTP, ALT is most strongly correlated with SD ($r = 0.33^{***}$) and slope and Asp (both with $r = -0.30^{***}$), followed by Dsoil and SNF (both with $r = -0.28^{***}$). As shown in Fig. 4, correlations among the different independent variables can also be observed.

From Figure 4, it can be observed that the factors significantly correlated with ALT vary across different permafrost types, and the strength of these correlations also differs. Overall, ALT shows a stronger correlation with soil properties in all the three permafrost regions. Except for the soil properties, ALT is more closely related to atmospheric temperature in the CAP regions, while in the SCAP and the QTP region, it exhibits a higher correlation with topographic factors.

https://doi.org/10.5194/egusphere-2026-841
Preprint. Discussion started: 17 June 2026

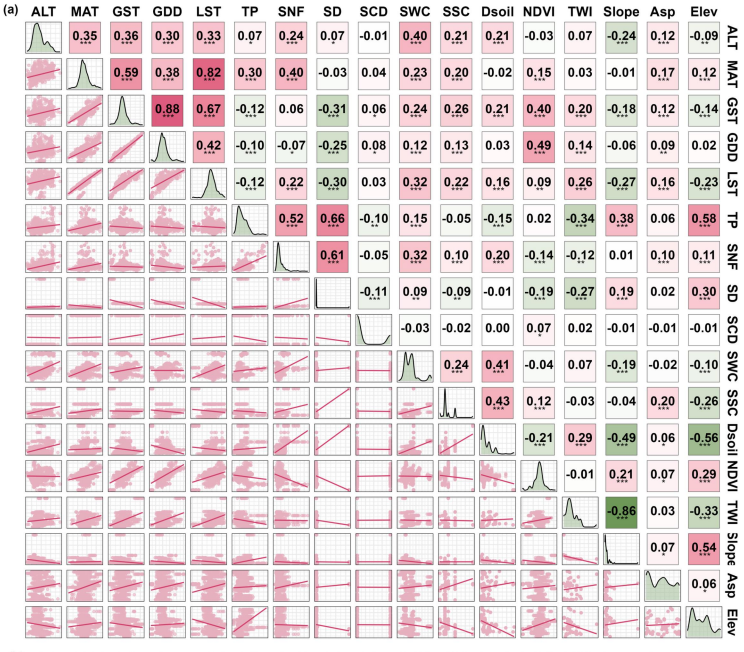

1

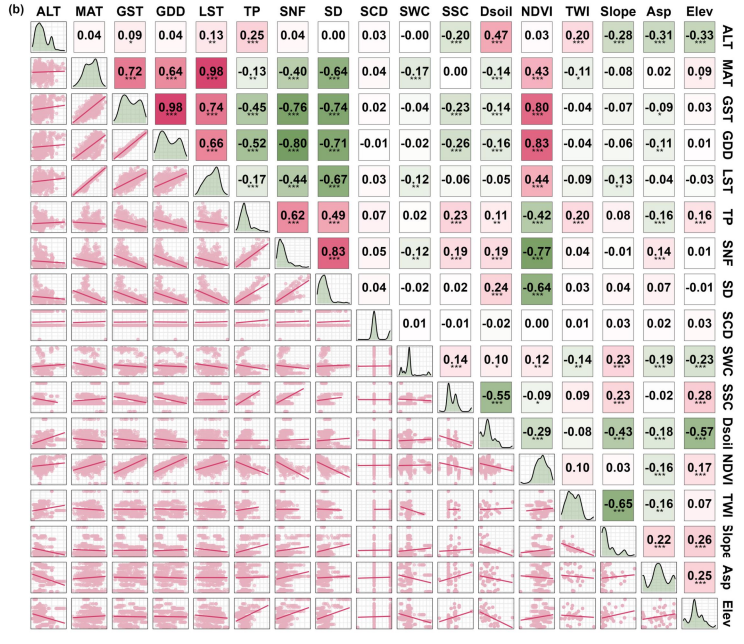

2

https://doi.org/10.5194/egusphere-2026-841
Preprint. Discussion started: 17 June 2026

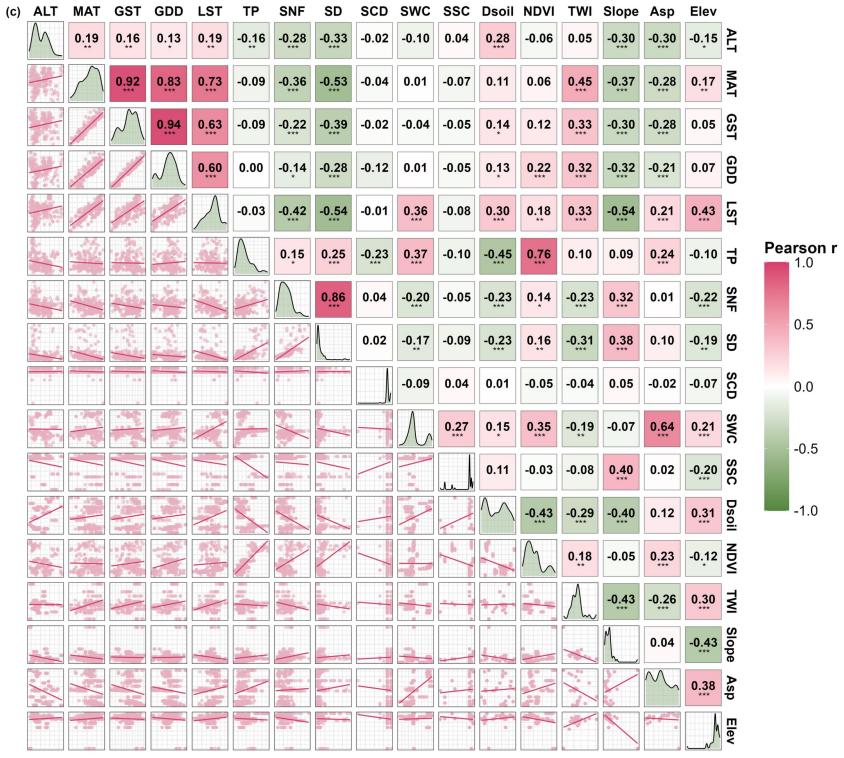

Fig. 4 Hot figures of Spearman correlation between ALT and each selected environmental factors for Circum-Arctic permafrost region (a), Sub-Circum-Arctic (b) and Qinghai-Tibetan Plateau (c) regions

3.4 Importance degree of environmental factors on ALT changes

The relative importance of each environmental factor, based on the XGBoost analysis, is presented in Figure 5. In the CAP region, among the selected factors, the four most influential variables affecting ALT variation are GDD, SSC, GST, and SWC. In contrast, in the SCAP, the SCD is the most critical factor influencing ALT variation, followed by Dsoil, SSC, and GST. In the QTP region, the dominant factors controlling ALT variation are Slope, Asp, Dsoil, and the TWI (Fig. 5). These findings indicate that in CAP regions where are colder than other regions, temperature-related variables and soil properties are the primary controls on ALT, while the influence of

https://doi.org/10.5194/egusphere-2026-841
Preprint. Discussion started: 17 June 2026

SCD is minimal. Conversely, in warmer SCAP regions, the SCD exert the strongest influence on ALT, followed by soil characteristics, whereas the relative importance of temperature factors is lower. In high-elevation permafrost areas, topographic factors are the dominant controls on ALT, followed by soil properties.

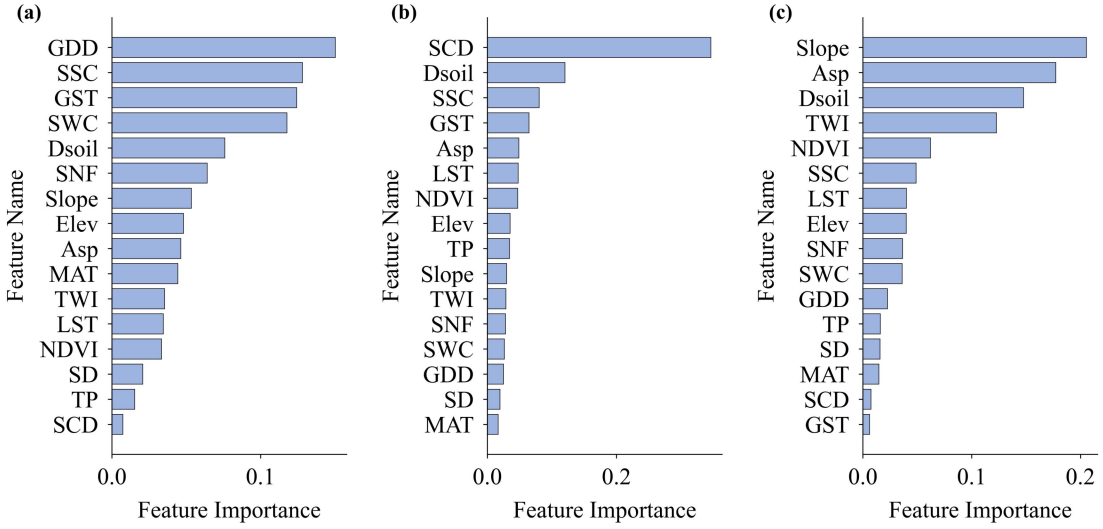

Fig. 5 Feature importance in affecting ALT in Circum-Arctic permafrost region (a), Sub-Circum-Arctic (b) and Qinghai-Tibetan Plateau (c) regions

3.5 Driving mechanism of environmental factors on ALT changes

The PLS-PM revealed that in the CAP region, the ALT driving mechanism model achieved GOF= 0.40 and R^2=0.34. Soil properties and temperature exerted the strongest influences on ALT, with correlation coefficients of r = 0.38*** and r = 0.35***, respectively. Precipitation also showed a positive effect on ALT in this region, whereas topography, snow depth, and NDVI exerted negative effects. From the total effect of each factor on ALT, we see that soil properties show the highest total effect value and followed by temperature and precipitation (Fig. 6a).

In the SCAP, the PLS-PM model performed better, with a GOF= 0.51 and R^2= 0.36, which is higher than those for the CAP and the QTP permafrost region.

https://doi.org/10.5194/egusphere-2026-841
Preprint. Discussion started: 17 June 2026

Topography, precipitation, NDVI, and soil depth directly influenced ALT, while air temperature affected ALT indirectly through multiple pathways. Topography had the greatest total effect and a negative influence ($r = –0.41^{***}$), followed by precipitation ($r = 0.40^{***}$) and NDVI ($r = 0.31^{***}$). The total effect of topography (-0.40) is higher than precipitation (0.37) and NDVI (0.31) (Fig. 6b).

For the QTP permafrost region, the PLS-PM yielded a GOF=0.50 but a relatively lower R^2 =0.25, indicating a weaker explanatory capacity for ALT changes compared with the CAP and SCAP regions. On the QTP, aspect, soil, NDVI, and snowfall directly affected ALT. Among these, aspect showed the strongest negative effect ($r = –0.51^{***}$), while soil properties exhibited the strongest positive effect ($r = 0.40^{***}$). Soil had the largest total effect on ALT (0.40), followed by aspect (–0.34) (Fig. 6c).

PLS-PM analysis reveals that across distinct permafrost types, the mechanisms governing energy distribution vary considerably due to pronounced differences in environmental conditions. The strength of interactions among key factors also differs substantially between these regions. As a result, both the pathways through which these factors influence ALT and the magnitude of their effects exhibit significant variation depending on permafrost type.

Comprehensive validation results for the PLS-PM models across the three permafrost regions (CAP, SCAP, and QTP) are provided in the Supplementary Materials. These include bootstrap tests of path coefficients and total effects (with standard errors and 95% confidence intervals), composite reliability (CR), average variance extracted (AVE), the heterotrait–monotrait ratio (HTMT), and effect-size analyses (*Cohen's* f^2), all reported in region-specific tables. Collectively, these diagnostics confirm the reliability and robustness of the inferred driving mechanisms.

https://doi.org/10.5194/egusphere-2026-841
Preprint. Discussion started: 17 June 2026

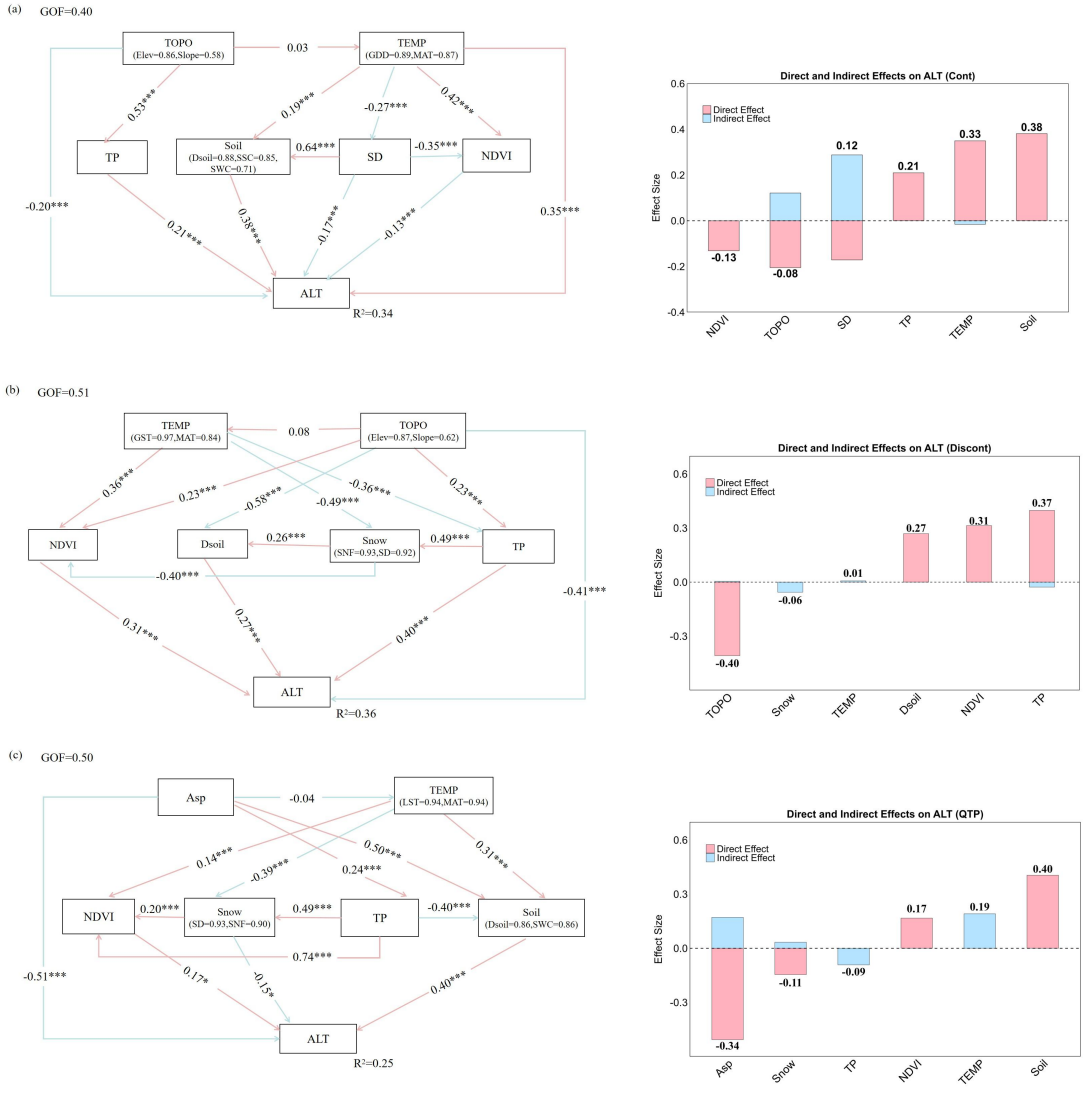

Fig. 6 PLS-SEM results of driving mechanisms of ALT for Circum-Arctic permafrost region (a), Sub-Circum-Arctic permafrost region (b) and Qinghai Tibet plateau (c)

https://doi.org/10.5194/egusphere-2026-841
Preprint. Discussion started: 17 June 2026

4. Discussion

4.1 The different trend of ALT in different monitoring sites

Based on long-term monitoring data, most permafrost sites (60%) exhibited an increasing trend in ALT, indicating widespread permafrost degradation. Similar patterns have been documented in recent studies (Yang et al., 2024; Liu et al., 2024). The 40% monitoring sites show decreasing trend of ALT may because that the warming climate not yet be sufficient to induce widespread permafrost degradation in these areas. Although high-latitude regions have experienced markedly greater warming than other parts of the world (Peng et al., 2023), their temperatures still fall within the range that supports permafrost formation. Consequently, permafrost degradation is most pronounced in mid- to high-latitude zones as well as in high-elevation areas (Peng et al., 2023) which is correspond to SCAP and QTP regions (Fig. 3).

The distinct ALT trend patterns among the CAP, SCAP, and QTP can be explained by hydrothermal condition variations between high and low latitudes. Some of these hydrothermal processes are regulated by topography, which drastically modifies zonal patterns and results in substantial geographic variability (Irrgang et al., 2025; Ran et al., 2022).Meteorological factors such as air temperature and precipitation generally increase with decreasing latitude (Wang et al., 2022; Yang et al., 2024). It is important to acknowledge that ALT thickening is an inherently slow process. Under otherwise stable conditions, the impact of rising air temperature on ALT deepening is relatively constrained, as temperatures do not increase monotonically or remain persistently high but fluctuate gradually over time. Such diurnal and irregular temperature variations exert only limited influence on soil heat transfer (Groenke et al., 2024).

https://doi.org/10.5194/egusphere-2026-841
Preprint. Discussion started: 17 June 2026

4.2 The different driving mechanism of ALT in different permafrost regions

Due to substantial differences in environmental conditions, the driving mechanisms of ALT vary across permafrost types. As shown in Figure 4, the correlations between ALT and its influencing factors differ notably among permafrost zones, consistent with previous research (Jorgenson et al., 2010; Yang et al., 2024; Peng et al., 2023). These correlations represent statistical associations under the combined influence of multiple variables; thus, they reflect regional differences in climate, vegetation, and the physicochemical properties of frozen ground, all of which alter the strength of interactions among factors and lead to distinct correlation patterns (Smith et al., 2022). However, correlation analysis alone cannot identify the dominant drivers of ALT, as it merely quantifies associations rather than disentangling the relative contribution of each factor. The XGBoost method effectively addresses this limitation by ranking the importance of environmental variables, and the resulting patterns are closely linked to regional environmental characteristics. For instance, in high-latitude, low-temperature continuous permafrost zones, temperature-related variables exert the strongest influence on ALT. In contrast, in discontinuous permafrost zones with relatively abundant snowfall, snow-related variables become more critical (Wang et al., 2022; Yang et al., 2024). On the QTP region, where high elevation is the defining feature, topographic factors play a key role in shaping ALT variability. Moreover, the PLS–SM analysis reveals how multiple factors interact to affect ALT and clarifies the causal pathways involved, while path analysis further distinguishes the direct and indirect effects of each factor.

The site-scale focus of this study constitutes a key characteristic that distinguishes the driving mechanisms of ALT from those identified in previous research (Peng et al., 2023). At broad spatial scales, differences in solar radiation across latitudes serve as the dominant driver of permafrost characteristics. At the site

https://doi.org/10.5194/egusphere-2026-841
Preprint. Discussion started: 17 June 2026

scale, however, local site conditions—such as topography, soil properties, and vegetation characteristics—become the primary factors influencing permafrost features (Guglielmin et al., 2014; Luo et al., 2023). This demonstrates that the drivers of ALT exhibit distinct scale dependence and must be analyzed separately across different spatial scales.

4.3 The total effect of environmental factors in influencing ALT

4.3.1 Temperature

When considering the site scale, temperature is not the leading factor in determining ALT. At regional scales, air temperature is the primary driver of permafrost degradation. On a broader scale, ALT is a function of both solar radiation and temperature, which are themselves influenced by elevation and latitude. At finer scales, variations in ALT are further shaped by factors such as topography, soil properties and micro-relief (Smith et al., 2022). However, the transfer of energy from the atmosphere to the soil is a highly complex process, influenced by vegetation, snow cover, surface litter, humus, and the physical and chemical properties of the soil (Juszak et al., 2014; Varlamov et al., 2019).

The GST must be considered when analyzing the effects of air temperature on ALT. Although numerous studies have identified an increase in mean annual air temperature as a primary driver of ALT increase, some scholars have also highlighted a close relationship between air temperature and soil temperature at various depth (Brown et al., 2000; Dobinski, 2011; Yang et al., 2024;). While the annual minimum temperature primarily influences permafrost temperatures during the winter, the annual maximum temperature typically has a transient (pulse-like) effect on ALT, as sustained high temperatures are rare, limiting their overall impact. Both mean annual

https://doi.org/10.5194/egusphere-2026-841
Preprint. Discussion started: 17 June 2026

temperature and mean GST may directly influence ALT and should be considered as latent variables for mechanistic analysis.

4.3.2 Soil

At the site scale, soil properties exert a stronger control on ALT than air temperature (Fig. 6). In permafrost regions, ALT is primarily governed by soil characteristics because incoming solar radiation is transmitted downward through the soil column, which mediates its influence on subsurface thermal regimes. Consequently, soil thermal conductivity directly determines the depth of seasonal thaw. Given the large variation in thermal conductivity among different media, factors such as soil sand content and soil moisture substantially affect heat conduction and phase-change dynamics (Huang et al., 2000). Soil properties regulate key thermal parameters—including thermal conductivity, heat capacity, moisture retention, and latent-heat effects—thereby controlling the magnitude and rate of heat flux through the permafrost profile. Clay and silt contents of the soil were initially considered but were ultimately excluded to avoid issues of collinearity. Their inclusion would have complicated the interpretation of results without contributing meaningful explanatory power. Furthermore, the influence of soil organic carbon and peat layer thickness on permafrost dynamics is indirectly captured by SWC, as these factors jointly modulate the soil's hydrothermal properties.

Fluctuations in surface temperature propagate downward as attenuating thermal waves, implying that changes in air temperature do not immediately affect deeper ground temperatures. Following a surface temperature perturbation, the resulting thermal anomaly propagates downward through successive soil layers, with both the velocity and depth of propagation depending on the thermal conductivity of the medium (Peng et al., 2023).

https://doi.org/10.5194/egusphere-2026-841
Preprint. Discussion started: 17 June 2026

4.3.3 Vegetation

Vegetation exerts varying effects on ALT across different permafrost regions, though the intensity of these effects differs by land cover type and permafrost region (Wang and Peng, 2023). Vegetation plays a key role in mitigating ALT by reducing the amount of solar radiation reaching the ground surface, thereby lowering ground temperatures. The vegetation canopy also impacts shading, snow accumulation, and the depth of the surface organic layer (Atchley et al., 2016; Loranty et al., 2018). The influence of vegetation is relatively small and negligible in both the CAP and QTP regions. In contrast, its overall effect ranks second in the SCAP region. This difference arises because the CAP, with its lower temperatures, is dominated by shrubs, while the QTP is primarily covered by bare land and grassland (Wu and Zhang, 2010). Compared with shrubs, herbs, and bare ground, forests have a lower surface albedo, which cools the soil and consequently decreases ALT (Fig. 2 and 3). The lower vegetation density in the CAP and QTP explains their limited impact on ALT (Yang et al., 2024).

4.3.4 Snow cover

At the site scale, the influence of snow cover on ALT is negligible (Fig. 6). Changes in snow cover conditions have been identified as a factor affecting shorter time scale (interannual) variations in soil temperatures (Frauenfeld et al. 2004). During the cold season, snow acts as an effective insulator that limits heat loss from the ground and buffers the influence of air temperature fluctuations on the ground thermal regime by slowing the freeze-thaw processes in the active layer (Osterkamp and Romanovsky, 1997; Taylor et al. 2006). However, the effect of snow depth on soil temperature is influenced by multiple factors, particularly the timing of the first snowfall, snow cover duration, and the snow depth. Research indicates that a

https://doi.org/10.5194/egusphere-2026-841
Preprint. Discussion started: 17 June 2026

significant insulating effect typically requires a minimum snow depth of around 20-50 cm with specific thresholds varying by area (Goncharova et al. 2019; Taylor and Jones 1990). Generally, a relatively thin snow cover mainly cools the ground surface in winter, because a relatively high surface albedo prevents the soil from absorbing solar long-wave radiation. Notably, ALT was measured in autumn, indicating that snow cover indirectly influences the subsequent year's ALT by affecting winter soil temperature.

4.4 Limitations

This study has two primary limitations that may influence the accuracy of its results. First, the data used in this research are mainly sourced from multiple databases (CALM and GTN-P) as well as various published studies. Due to the lack of standardized data collection methods and tools, the accuracy of the ALT measurements may vary across sources, potentially introducing inherent errors into the dataset. However, considering the scarcity of in situ observations and the relatively low accuracy of simulated data, the data sources adopted here remain the most reliable options currently available.

Second, most of the environmental variables employed in this study are derived from remote sensing, using pixel values extracted at monitoring site locations. Although uniform site-based survey data would be ideal, such data are difficult to obtain across large spatial scales and long temporal spans. Remote sensing therefore provides the most effective means of capturing and understanding spatiotemporal patterns of geographic factors at broad scales.

https://doi.org/10.5194/egusphere-2026-841
Preprint. Discussion started: 17 June 2026

5. Conclusions

Based on ALT monitoring data across the Northern Hemisphere, this study analyzed the temporal dynamics of ALT at the site scale and explored the underlying climatic, soil, topography and vegetation-related drivers. To better characterize spatial heterogeneity, Northern Hemisphere permafrost was categorized into three types: CAP, SCAP, and the QTP permafrost regions. The key findings are as follows:

Most monitoring sites across the Northern Hemisphere show an increasing trend in ALT, indicating widespread permafrost degradation. The XGBoost model results indicate that the relative importance of environmental factors influencing ALT varies by permafrost type. Soil properties show high importance across all three permafrost zones. Beyond this common factor, temperature plays a more prominent role in the CAP regions, snowfall is more influential in the SCAP regions, and topographic factors are the most significant in the QTP region. The PLS-PM results show that at the site level, air temperature is not the dominant factor controlling ALT variability; instead, soil properties exhibit a stronger and more consistent influence across all three permafrost regions. Vegetation factors, particularly NDVI, exert a notable positive effect on ALT mainly within the SCAP region, while the influence of snowfall on ALT is generally weak in all the three permafrost regions. Topographic conditions show the strongest negative effect on ALT in both the SCAP and QTP regions. These observational records enable a more detailed and robust understanding of permafrost degradation trajectories and their driving mechanisms at fine spatial scales.

https://doi.org/10.5194/egusphere-2026-841
Preprint. Discussion started: 17 June 2026

CRediT authorship contribution statement

Yutong Lin: Writing – original draft, Methodology, Investigation, Funding acquisition, Formal analysis, Data curation. **Bo Zhang**: Writing – review & editing, Formal analysis, Data curation. **Haoqi Suo**: Writing – review & editing, Methodology, Investigation, Funding acquisition, Conceptualization. **Meng Guo**: Writing – review & editing, Funding acquisition, Formal analysis, Supervision.

Declaration of competing interest

The authors declare that they have no known competing financial interests or personal relationships that could have appeared to influence the work reported in this paper.

Acknowledgements

This work was supported by the National Natural Science Foundation of China [Grant No. 42371098].

Data availability

The datasets used in this study are publicly available. ALT data can be accessed via the CALM network (https://www2.gwu.edu/~calm/), the GTN-P database (http://gtnpdatabase.org/activelayers). Global Monitoring and Modelling Study Group (GIMMS) data is available at https://daac.ornl.gov/. The ASTER GDEM V3 dataset were downloaded from http://www.gscloud.cn. Soil Grids 250m were downloaded from https://isric.org/. Harmonized World Soil Database v2.0 were downloaded from https://www.fao.org/soils-portal/en/.

https://doi.org/10.5194/egusphere-2026-841
Preprint. Discussion started: 17 June 2026

References

Atchley, A. L., Coon, E. T., Painter, S. L., Harp, D. R., and Wilson, C. J.: Influences and interactions of inundation, peat, and snow on active layer thickness, Geophys. Res. Lett., 43, 5116 – 5123, https://doi.org/10.1002/2016GL068550, 2016.

Berner, L. T., Massey, R., Jantz, P., Forbes, B. C., Macias-Fauria, M., Myers-Smith, I., Kumpula, T., Gauthier, G., Andreu-Hayles, L., Gaglioti, B. V., Burns, P., Zetterberg, P., D' Arrigo, R., and Goetz, S. J.: Summer warming explains widespread but not uniform greening in the Arctic tundra biome., Nat. Commun., 11, 4621, https://doi.org/10.1038/s41467-020-18479-5, 2020.

Biskaborn, B. K., Lanckman, J.-P., Lantuit, H., Elger, K., Streletskiy, D. A., Cable, W. L., and Romanovsky, V. E.: The new database of the Global Terrestrial Network for Permafrost (GTN-P), Earth Syst. Sci. Data, 7, 245 – 259, https://doi.org/10.5194/essd-7-245-2015, 2015.

Brown, J., Ferrians, O. J., Heginbottom, J. A., and Melnikov, E. S.: Circum-Arctic map of permafrost and ground-ice conditions, USGS Rep., 2, https://doi.org/10.3133/cp45, 1997.

Brown, J., Hinkel, K. M., and Nelson, F. E.: The circumpolar active layer monitoring (calm) program: Research designs and initial results, Polar Geogr., 24, 166 – 258, https://doi.org/10.1080/10889370009377698, 2000.

Chen, R. H., Tabatabaeenejad, A., and Moghaddam, M.: Retrieval of Permafrost Active Layer Properties Using Time-Series P-Band Radar Observations, IEEE Trans. Geosci. Remote Sens., 57, 6037 – 6054, https://doi.org/10.1109/TGRS.2019.2903935, 2019.

Chen, T. and Guestrin, C.: XGBoost: A Scalable Tree Boosting System, in: Proceedings of the 22nd ACM SIGKDD International Conference on Knowledge Discovery and Data Mining, KDD ' 16: The 22nd ACM SIGKDD International Conference on Knowledge Discovery and Data Mining, 785 – 794, https://doi.org/10.1145/2939672.2939785, 2016.

Cline, D. W.: Snow surface energy exchanges and snowmelt at a continental, midlatitude Alpine site, Water Resour. Res., 33, 689 – 701, https://doi.org/10.1029/97WR00026, 1997.

Dobinski, W.: Permafrost, Earth-Sci. Rev., 108, 158 – 169, https://doi.org/10.1016/j.earscirev.2011.06.007, 2011.

Du, R., Peng, X., Frauenfeld, O. W., Sun, W., Liang, B., Chen, C., Jin, H., and Zhao, Y.: The role of peat on permafrost thaw based on field observations, CATENA, 208, 105772, https://doi.org/10.1016/j.catena.2021.105772, 2022.

FAO and IIASA. 2023. Harmonized World Soil Database Version 2.0. Rome and Laxenburg. https://doi.org/10.4060/cc3823en.

Frauenfeld, O. W., Zhang, T. J., Barry, R. G., and Gilichinsky, D.: Interdecadal changes in seasonal freeze and thaw depths in Russia - art. no. D05101, J. Geophys. Res.-Atmospheres, 109, D05101, https://doi.org/10.1029/2003JD004245, 2004.

Goncharova, O. Yu., Matyshak, G. V., Epstein, H. E., Sefilian, A. R., and Bobrik, A. A.: Influence of snow cover on soil temperatures: Meso- and micro-scale topographic effects (a case study from the northern West Siberia discontinuous permafrost zone), CATENA, 183, 104224, https://doi.org/10.1016/j.catena.2019.104224, 2019.

Groenke, B., Langer, M., Miesner, F., Westermann, S., Gallego, G., and Boike, J.: Robust Reconstruction of Historical Climate Change From Permafrost Boreholes, J. Geophys. Res.-Earth Surf., 129, e2024JF007734, https://doi.org/10.1029/2024JF007734, 2024.

https://doi.org/10.5194/egusphere-2026-841
Preprint. Discussion started: 17 June 2026

Guglielmin, M., Dalle Fratte, M., and Cannone, N.: Permafrost warming and vegetation changes in continental Antarctica, Environ. Res. Lett., 9, 045001, https://doi.org/10.1088/1748-9326/9/4/045001, 2014.
Günther, F., Overduin, P. P., Yakshina, I. A., Opel, T., Baranskaya, A. V., and Grigoriev, M. N.: Observing Muostakh disappear: permafrost thaw subsidence and erosion of a ground-ice-rich island in response to arctic summer warming and sea ice reduction, The Cryosphere, 9, 151 – 178, https://doi.org/10.5194/tc-9-151-2015, 2015.
Hair, J. F., Risher, J. J., Sarstedt, M., and Ringle, C. M.: When to use and how to report the results of PLS-SEM, Eur. Bus. Rev., 31, 2 – 24, https://doi.org/10.1108/EBR-11-2018-0203, 2019.
Hamed, K. H. and Ramachandra Rao, A.: A modified Mann-Kendall trend test for autocorrelated data, J. Hydrol., 204, 182 – 196, https://doi.org/10.1016/S0022-1694(97)00125-X, 1998.
Hengl, T., Jesus, J. M. de, Heuvelink, G. B. M., Gonzalez, M. R., Kilibarda, M., Blagotić, A., Shangguan, W., Wright, M. N., Geng, X., Bauer-Marschallinger, B., Guevara, M. A., Vargas, R., MacMillan, R. A., Batjes, N. H., Leenaars, J. G. B., Ribeiro, E., Wheeler, I., Mantel, S., and Kempen, B.: SoilGrids250m: Global gridded soil information based on machine learning, PLOS ONE, 12, e0169748, https://doi.org/10.1371/journal.pone.0169748, 2017.
Heginbottom, J. A.: Permafrost mapping: a review, Prog. Phys. Geogr. Earth Environ., 26, 623 – 642, https://doi.org/10.1191/0309133302pp355ra, 2002.
Huang, S., Pollack, H. N., and Shen, P.-Y.: Temperature trends over the past five centuries reconstructed from borehole temperatures, Nature, 403, 756 – 758, https://doi.org/10.1038/35001556, 2000.
Muñoz-Sabater, J.: ERA5-Land monthly averaged data from 1950 to present, Copernicus Climate Change Service (C3S) Climate Data Store (CDS), https://doi.org/10.24381/cds.68d2bb30, 2019.
Muñoz Sabater, J., Comyn-Platt, E., Hersbach, H., Bell, B., Berrisford, P., Biavati, G., Horányi, A., Nicolas, J., Peubey, C., Radu, R., Rozum, I., Schepers, D., Simmons, A., Soci, C., Dee, D., Thépaut, J.-N., Cagnazo, C., and Cucchi, M.: ERA5-land post-processed daily-statistics from 1950 to present, Copernicus Climate Change Service (C3S) Climate Data Store (CDS), https://doi.org/10.24381/cds.e9c9c792, 2024..
Jevšenak, J.: New features in the dendroTools R package: Bootstrapped and partial correlation coefficients for monthly and daily climate data, Dendrochronologia, 63, 125753, https://doi.org/10.1016/j.dendro.2020.125753, 2020.
Jin, H., Jin, X., He, R., Luo, D., Chang, X., Wang, S., Marchenko, S. S., Yang, S., Yi, C., Li, S., and Harris, S. A.: Evolution of permafrost in China during the last 20 ka, Sci. China Earth Sci., 62, 1207 – 1223, https://doi.org/10.1007/s11430-018-9272-0, 2019.
Jilin Yang, Jinwei Dong, Xiangming,Xiao, et al. Divergent shifts in peak photosynthesis timing of temperate and alpine grasslands in China. Remote Sensing of Environment, 2019, 233. https://doi.org/10.1016/j.rse.2019.111395.
Jin, H.-J., Wu, Q.-B., and Romanovsky, V. E.: Degrading permafrost and its impacts, Adv. Clim. Change Res., 12, 1 – 5, https://doi.org/10.1016/j.accre.2021.01.007, 2021.
Jorgenson, M. T., Romanovsky, V., Harden, J., Shur, Y., O' Donnell, J., Schuur, E. A. G., Kanevskiy, M., and Marchenko, S.: Resilience and vulnerability of permafrost to climate changeThis article is one of a selection of papers from The Dynamics of Change in Alaska' s Boreal Forests: Resilience and Vulnerability in Response to Climate Warming., Can. J. For. Res., 40, 1219 – 1236, https://doi.org/10.1139/X10-060, 2010.

https://doi.org/10.5194/egusphere-2026-841
Preprint. Discussion started: 17 June 2026

Juszak, I., Erb, A. M., Maximov, T. C., and Schaepman-Strub, G.: Arctic shrub effects on NDVI, summer albedo and soil shading, Remote Sens. Environ., 153, 79–89, https://doi.org/10.1016/j.rse.2014.07.021, 2014.

Liu, Z., Kimball, J. S., Ballantyne, A., Watts, J. D., Natali, S. M., Rogers, B. M., Yi, Y., Klene, A. E., Moghaddam, M., Du, J., and Zona, D.: Widespread deepening of the active layer in northern permafrost regions from 2003 to 2020, Environ. Res. Lett., 19, 014020, https://doi.org/10.1088/1748-9326/ad0f73, 2024.

Loranty, M. M., Abbott, B. W., Blok, D., Douglas, T. A., Epstein, H. E., Forbes, B. C., Jones, B. M., Kholodov, A. L., Kropp, H., Malhotra, A., Mamet, S. D., Myers-Smith, I. H., Natali, S. M., O'Donnell, J. A., Phoenix, G. K., Rocha, A. V., Sonnentag, O., Tape, K. D., and Walker, D. A.: Reviews and syntheses: Changing ecosystem influences on soil thermal regimes in northern high-latitude permafrost regions, Biogeosciences, 15, 5287–5313, https://doi.org/10.5194/bg-15-5287-2018, 2018.

Luo, D., Wu, Q., Jin, H., Marchenko, S. S., Lü, L., and Gao, S.: Recent changes in the active layer thickness across the northern hemisphere, Environ. Earth Sci., 75, 555, https://doi.org/10.1007/s12665-015-5229-2, 2016.

LUO, D., JIN, H., WU, Q., MAKARIEVA, O., TIAN, S., KANG, J., WANG, J., PENG, X., DOBIŃSKI, W., and CHEN, F.: Active layer thickness （ALT） in permafrost regions under natural/undisturbed state： a review, J. Glaciol. Geocryol., 45, 558–574, https://doi.org/10.7522/j.issn.1000-0240.2023.0043, 2023.

Marquardt, D. W.: Generalized Inverses, Ridge Regression, Biased Linear Estimation, and Nonlinear Estimation, Technometrics, 12, 591–612, https://doi.org/10.1080/00401706.1970.10488699, 1970.

Mishra, U. and Riley, W. J.: Active-Layer Thickness across Alaska: Comparing Observation-Based Estimates with CMIP5 Earth System Model Predictions, Soil Sci. Soc. Am. J., 78, 894–902, https://doi.org/10.2136/sssaj2013.11.0484, 2014.

NASA, METI, AIST, Japan Spacesystems and U.S., Japan ASTER Science Team: ASTER Global Digital Elevation Model V003, NASA EOSDIS Land Processes DAAC, https://doi.org/10.5067/ASTER/ASTGTM.003, 2018.

Nelson, F. E., Shiklomanov, N. I., and Mueller, G. R.: Variability of active-layer thickness at multiple spatial scales, north-central Alaska, USA, Arct. Antarct. Alp. Res., 31, 179–186, https://doi.org/10.2307/1552606, 1999.

Obu, J.: How Much of the Earth's Surface is Underlain by Permafrost?, J. Geophys. Res. Earth Surf., 126, e2021JF006123, https://doi.org/10.1029/2021JF006123, 2021.

Osterkamp, T. E. and Romanovsky, V. E.: Freezing of the Active Layer on the Coastal Plain of the Alaskan Arctic, Permafr. Periglac. Process., 8, 23–44, https://doi.org/10.1002/(SICI)1099-1530(199701)8:1%253C23::AID-PPP239%253E3.0.CO;2-2, 1997.

Pinzon, J. E. and Tucker, C. J.: A Non-Stationary 1981–2012 AVHRR NDVI3g Time Series, Remote Sens., 6, 6929–6960, https://doi.org/10.3390/rs6086929, 2014.

Peng, X., Zhang, T., Frauenfeld, O. W., Mu, C., Wang, K., Wu, X., Guo, D., Luo, J., Hjort, J., Aalto, J., Karjalainen, O., and Luoto, M.: Active Layer Thickness and Permafrost Area Projections for the 21st Century, Earths Future, 11, e2023EF003573, https://doi.org/10.1029/2023EF003573, 2023.

Post, E., Alley, R. B., Christensen, T. R., Macias-Fauria, M., Forbes, B. C., Gooseff, M. N., Iler, A., Kerby, J. T., Laidre, K. L., Mann, M. E., Olofsson, J., Stroeve, J. C., Ulmer, F., Virginia, R. A., and Wang, M.: The polar regions in a 2° C warmer world, Sci. Adv., https://doi.org/10.1126/sciadv.aaw9883, 2019.

https://doi.org/10.5194/egusphere-2026-841
Preprint. Discussion started: 17 June 2026

Ran, Y., Li, X., Cheng, G., Che, J., Aalto, J., Karjalainen, O., Hjort, J., Luoto, M., Jin, H., Obu, J., Hori, M., Yu, Q., and Chang, X.: New high-resolution estimates of the permafrost thermal state and hydrothermal conditions over the Northern Hemisphere, Earth Syst. Sci. Data, 14, 865–884, https://doi.org/10.5194/essd-14-865-2022, 2022.

Rantanen, M., Kämäräinen, M., Luoto, M., and Aalto, J.: Manifold increase in the spatial extent of heatwaves in the terrestrial Arctic, Commun. Earth Environ., 5, 570, https://doi.org/10.1038/s43247-024-01750-8, 2024.

Reyes, F. R. and Lougheed, V. L.: Rapid Nutrient Release from Permafrost Thaw in Arctic Aquatic Ecosystems, Arct. Antarct. Alp. Res., 47, 35–48, https://doi.org/10.1657/AAAR0013-099, 2015.

Schaefer, K., Zhang, T., Bruhwiler, L., and Barrett, A. P.: Amount and timing of permafrost carbon release in response to climate warming, TELLUS Ser. B-Chem. Phys. Meteorol., 63, 165–180, https://doi.org/10.1111/j.1600-0889.2011.00527.x, 2011.

Schaefer, K., Lantuit, H., Romanovsky, V. E., Schuur, E. A. G., and Witt, R.: The impact of the permafrost carbon feedback on global climate, Environ. Res. Lett., 9, 085003, https://doi.org/10.1088/1748-9326/9/8/085003, 2014.

Schuur, E. A. G., Bockheim, J., Canadell, J. G., Euskirchen, E., Field, C. B., Goryachkin, S. V., Hagemann, S., Kuhry, P., Lafleur, P. M., Lee, H., Mazhitova, G., Nelson, F. E., Rinke, A., Romanovsky, V. E., Shiklomanov, N., Tarnocai, C., Venevsky, S., Vogel, J. G., and Zimov, S. A.: Vulnerability of permafrost carbon to climate change: Implications for the global carbon cycle, BIOSCIENCE, 58, 701–714, https://doi.org/10.1641/B580807, 2008.

Schuur, E. A. G., McGuire, A. D., Schädel, C., Grosse, G., Harden, J. W., Hayes, D. J., Hugelius, G., Koven, C. D., Kuhry, P., Lawrence, D. M., Natali, S. M., Olefeldt, D., Romanovsky, V. E., Schaefer, K., Turetsky, M. R., Treat, C. C., and Vonk, J. E.: Climate change and the permafrost carbon feedback., Nature, 520, 171–179, https://doi.org/10.1038/nature14338, 2015.

Shen, T., Jiang, P., Ju, Q., Yu, Z., Chen, X., Lin, H., and Zhang, Y.: Changes in permafrost spatial distribution and active layer thickness from 1980 to 2020 on the Tibet Plateau, Sci. Total Environ., 859, 160381, https://doi.org/10.1016/j.scitotenv.2022.160381, 2023.

Shijin, W. and Xiaoqing, P.: Permafrost degradation services for Arctic greening, CATENA, 229, 107209, https://doi.org/10.1016/j.catena.2023.107209, 2023.

Smith, S. L., O'Neill, H. B., Isaksen, K., Noetzli, J., and Romanovsky, V. E.: The changing thermal state of permafrost, Nat. Rev. Earth Environ., 3, 10–23, https://doi.org/10.1038/s43017-021-00240-1, 2022.

Taylor, A. E., Wang, K., Smith, S. L., Burgess, M. M., and Judge, A. S.: Canadian Arctic Permafrost Observatories: Detecting contemporary climate change through inversion of subsurface temperature time series, J. Geophys. Res. Solid Earth, 111, 2004JB003208, https://doi.org/10.1029/2004JB003208, 2006.

Taylor, B. R. and Jones, H. G.: Litter decomposition under snow cover in a balsam fir forest, Can. J. Bot., 68, 112–120, https://doi.org/10.1139/b90-016, 1990.

Tenenhaus, M., Vinzi, V. E., Chatelin, Y. M., and Lauro, C.: PLS path modeling, Comput. Stat. Data Anal., 48, 159–205, https://doi.org/10.1016/j.csda.2004.03.005, 2005.

Varlamov, S. P., Skachkov, Y. B., and Skryabin, P. N.: Evolution of the thermal state of permafrost under climate warming in Central Yakutia, The Holocene, 29, 1401–1410, https://doi.org/10.1177/0959683619855959, 2019.

https://doi.org/10.5194/egusphere-2026-841
Preprint. Discussion started: 17 June 2026

Shiklomanov, N., Nelson, F., Streletskiy, D., and Hinkel, K.: The Circumpolar Active Layer Monitoring (CALM) Program: Data Collection, Management, and Dissemination Strategies, Proc. Ninth Int. Conf. Permafr., 2, 2008.

Walter Anthony, K., Schneider Von Deimling, T., Nitze, I., Frolking, S., Emond, A., Daanen, R., Anthony, P., Lindgren, P., Jones, B., and Grosse, G.: 21st-century modeled permafrost carbon emissions accelerated by abrupt thaw beneath lakes., Nat. Commun., 9, 3262, https://doi.org/10.1038/s41467-018-05738-9, 2018.

Wang, X., Song, C., Sun, X., Wang, J., Zhang, X., and Mao, R.: Soil carbon and nitrogen across wetland types in discontinuous permafrost zone of the Xiao Xing"an Mountains, northeastern China, CATENA, 101, 31 – 37, https://doi.org/10.1016/j.catena.2012.09.007, 2013.

Wang, X., Ran, Y., Pang, G., Chen, D., Su, B., Chen, R., Li, X., Chen, H. W., Yang, M., Gou, X., Jorgenson, M. T., Aalto, J., Li, R., Peng, X., Wu, T., Clow, G. D., Wan, G., Wu, X., and Luo, D.: Contrasting characteristics, changes, and linkages of permafrost between the Arctic and the Third Pole, Earth-Sci. Rev., 230, 104042, https://doi.org/10.1016/j.earscirev.2022.104042, 2022.

World Meteorological Organization (WMO): Guide to Instruments and Methods of Observation (WMO-No. 8), Volume II – Measurement of Cryospheric Variables, World Meteorological Organization (WMO), https://doi.org/10.59327/WMO/CIMO/2, 2024.

Wu, Q. and Zhang, T.: Changes in active layer thickness over the Qinghai – Tibetan Plateau from 1995 to 2007, J. Geophys. Res. Atmospheres, 115, 2009JD012974, https://doi.org/10.1029/2009JD012974, 2010.

Yang, Y., Wang, X., and Wang, T.: Permafrost Degradation Induces the Abrupt Changes of Vegetation NDVI in the Northern Hemisphere, Earths Future, 12, e2023EF004309, https://doi.org/10.1029/2023EF004309, 2024.

Yun, H., Zhu, Q., Tang, J., Zhang, W., Chen, D., Ciais, P., Wu, Q., and Elberling, B.: Warming, permafrost thaw and increased nitrogen availability as drivers for plant composition and growth across the Tibetan Plateau, Soil Biol. Biochem., 182, 109041, https://doi.org/10.1016/j.soilbio.2023.109041, 2023.

Zhang, G., Nan, Z., Wu, X., Ji, H., and Zhao, S.: The Role of Winter Warming in Permafrost Change Over the Qinghai – Tibet Plateau, Geophys. Res. Lett., 46, 11261 – 11269, https://doi.org/10.1029/2019GL084292, 2019.

Zhang, T.: Influence of the seasonal snow cover on the ground thermal regime: An overview, Rev. Geophys., 43, 2004RG000157, https://doi.org/10.1029/2004RG000157, 2005.

Zhang, T., Osterkamp, T. E., and Stamnes, K.: Effects of Climate on the Active Layer and Permafrost on the North Slope of Alaska, U.S.A., Permafr. Periglac. Process., 8, 45 – 67, https://doi.org/10.1002/(SICI)1099-1530(199701)8:1%253C45::AID-PPP240%253E3.0.CO2-K, 1997.